

## Quenching of Pairing Correlations – a Simple Model for Rotating Nuclei

**P. Quentin**<sup>1,2</sup>, **H. Lafchiev**<sup>3</sup>, **D. Samsøen**<sup>1</sup>, and  
**I. N. Mikhailov**<sup>4,5</sup>

<sup>1</sup>Centre d'Études Nucléaires de Bordeaux-Gradignan (CNRS-IN2P3 and Université Bordeaux I), Le Haut Vigneau BP 120, F-33175 Gradignan, France

<sup>2</sup>Theoretical Division, T-DO (Los Alamos National Laboratory), PO Box 1663, Los Alamos, NM 87545, USA

<sup>3</sup>Institute of Nuclear Research and Nuclear Energy, Bulgarian Academy of Sciences, Sofia 1784, Bulgaria

<sup>4</sup>Bogoliubov Laboratory of Theoretical Physics (Joint Institute of Nuclear Research), Joliot-Curie str. 6, 141980 Dubna (Moscow Region), Russia

<sup>5</sup>Centre de spectrométrie Nucléaire et de Spectrométrie de Masse, (CNRS-IN2P3 and Université Paris XI), Bât. 104, 91406 Orsay-Campus, France

### Abstract.

Adding a Kelvin momentum constraint to the Routhian HF equations one generates intrinsic vortical currents in the HF solution and it is found that one may simply reproduce in such a way the HFB dynamical properties of rotating nuclei. From the analogy between magnetic and rotating systems, one derives a model for the quenching of pairing correlations with rotation, introducing a critical angular velocity ( $\Omega_c$ ) – analogous to the critical field in superconductors – above which pairing vanishes. An important feature of this model is the existence of an universal dependence between the angular velocity  $\Omega$  and the intrinsic angular velocity  $\omega$ , where  $\Omega_c$  is playing an important role. Taking stock of this model, it is then shown that this dependence could be modelised by a simple two parameter formula, both parameters being completely determined from properties of the band-head (zero-spin) HFB solution. From calculation in five nuclei, the validity of this modelised Routhian approach is assessed. It is clearly shown to be very good in cases where the evolution of rotational properties is only governed by the coupling between the global rotation and the pairing-induced intrinsic vortical currents. It therefore provides a sound ground base for evaluating the importance of coupling of rotation with other modes (shape distortions, quasiparticle degrees of freedom).

## 1 Introduction

Dynamical effects of pairing correlations at finite spins could be very well represented indeed by an intrinsic flow being both non-deforming and counter-rotating (with respect to the global rotation) [1] (hereafter referred as I). This has been borne out from the study of rotational bands in three heavy nuclei chosen to represent rather different cases (as far as nucleon numbers, deformation, spin values or pairing correlation content are concerned). To achieve this, we have performed two sets of microscopic calculations under a Routhian-type constraint (namely including in the variational quantity for the rotating case a  $-\vec{\Omega} \cdot \vec{J}$  term with usual notation). The first calculations have included pairing correlations within the Hartree-Fock-Bogoliubov (HFB) formalism. The second ones were of the Hartree-Fock type (i.e., without any pairing correlations) with a double Routhian-type constraint, as presented in Refs. [2–4] which we will refer to below as HF+V calculations. The “measuring stick” for the latter was the so-called Kelvin circulation operator  $\hat{K}_1$  (see, e.g., Ref. [5]) which is well suited for the description of collective modes dubbed after Chandrasekhar as *S*-type ellipsoids [6].

The operator  $\hat{K}_1$  is the first component of the Kelvin circulation operator which writes in cartesian coordinates

$$\hat{K}_1 = -\hbar \left( q x_2 \frac{\partial}{\partial x_3} - \frac{1}{q} x_3 \frac{\partial}{\partial x_2} \right), \quad (1)$$

$q$  being the axis ratio  $a_3/a_2$ , where  $a_2, a_3$  are the semi-axis following the  $y, z$  axis. This definition corresponds to a double stretching of the angular momentum operator in both positions and momenta. When the expectation value of this operator is constrained, ellipsoidal vortical currents are generated in the plane perpendicular to the  $x$ -axis. This constraint  $-\omega \hat{K}_1$  (here the intrinsic angular velocity  $\omega$  is a kind of Lagrange multiplier) is similar to the angular momentum constraint  $-\Omega \hat{J}_1$ . The latter generates, as well known, rotational currents in the solution so that  $\langle \hat{J}_1 \rangle$  is a good measure for the collective rotation. When one uses both of them to constrain an HF solution, one generates in the solution intrinsic vortical and circular currents in the plane perpendicular to the  $x$ -axis and in the laboratory frame.

As it is well known, in the body-fixed rotating frame the circular currents generated by the angular momentum constraint disappear. This coordinate transformation between the laboratory and the rotating frames is a rotation with an angle  $\theta$  around the  $x$ -axis where the operator is  $T = R(\theta) = e^{i\theta J_1}$ . The transformation of the single-particle density matrix is

$$\rho = e^{-i\theta J_1} \tilde{\rho} e^{i\theta J_1}, \quad (2)$$

where  $\rho$  is the matrix in the laboratory frame and  $\tilde{\rho}$  is the matrix in the rotating frame.

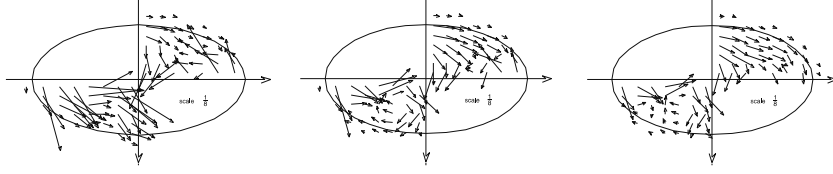


Figure 1. Current patterns in the body-fixed rotating frame for  $^{150}\text{Gd}$  at spin  $I=32\hbar$ : 1st column - HF approach, 2nd column - HF+vorticity approach, 3rd column - HFB+LN approach. The neutron currents are on the left bottom side, the proton ones are on the right upper side of the ellipses defining the deformed nuclear shape.

Similarly, there is frame of reference (denoted as the vortical frame) where both the intrinsic vortical and the circular currents disappear. The coordinate transformation between the laboratory and the vortical frames is a combination of 4 consecutive transformations conserving the volume – two rotations with corresponding angles  $\theta$  and  $\vartheta$  around the x-axis, transformation between an ellipsoid and sphere  $A(q)$  and the inverse transformation between a sphere and an ellipsoid –  $A(q)^{-1}$  [Ref. Chandrasekhar]. The operator of the transformation is  $T' = R(\theta) = e^{i\theta J_1} A(q) e^{i\vartheta J_1} A(q)^{-1}$ . In the vortical frame the single particle density matrix is denoted as  $\bar{\rho}$ .

Now, upon imposing via the Routhian double-constraint that the HF+V type of solutions should have the same  $\langle \hat{K}_1 \rangle$  expectation value at a given value of the spin  $I$  as those corresponding to the HFB calculations, it has been demonstrated in I that both calculations yielded the same rotational properties. One sees on Figure 1 (taken from I), that in the HF+V solution for the Yrast SD band of  $^{150}\text{Gd}$ , the intrinsic currents perpendicular to the x-axis, are very close indeed to the intrinsic currents in the HFB solution.

The dynamical equations of motion of these two approaches could be described as follows:

$$i\hbar \frac{\partial \mathfrak{R}}{\partial t} = [H_{\text{hfb}}, \mathfrak{R}] \quad (3)$$

$$i\hbar \frac{\partial \rho}{\partial t} = [h, \rho] = [\Omega \hat{J}_1 + \omega \hat{K}_1, \rho] . \quad (4)$$

When one take the subset of the time-dependent HFB system of equations which corresponds to the upper-left block  $\mathfrak{R}_{11}$  (when the generalized density matrix  $\mathfrak{R}$  is presented through its usual 2x2 matrix expression) one obtains

$$i\hbar \frac{\partial \mathfrak{R}_{(11)}}{\partial t} = [H, \mathfrak{R}]_{(11)} = i\hbar \frac{\partial \rho}{\partial t} = [h, \rho] - (\Delta \kappa^* - \kappa \Delta^*) = [\Omega_{\text{hfb}} \hat{J}_1, \rho] . \quad (5)$$

Taking into account that, through constraints, some collective motion problems could be described with static equations in the appropriate frame of reference, we write the static equations of motion (5) and the HF+V approaches as

follows [Hristo these]:

$$i\hbar \frac{\partial \tilde{\rho}}{\partial t} = 0 = [\tilde{h} - \Omega \hat{J}_1, \tilde{\rho}] - (\Delta\kappa^* - \kappa\Delta^*), \quad (6)$$

$$i\hbar \frac{\partial \bar{\rho}}{\partial t} = 0 = [\bar{h} - \Omega \hat{J}_1, \bar{\rho}] - [\omega \hat{K}_1, \bar{\rho}]. \quad (7)$$

Here the HFB equations of motion are in the rotating frame and the HF+ V equations of motion are in the intrinsic vortical frame.

Analyzing these two equations and the current patterns at Figure 1 it is easy to see that the term which explicitly generates intrinsic vortical currents in the solution is the second term in both of them. This term is missing in the equations of motion of the cranked HF approach:

$$i\hbar \frac{\partial \tilde{\rho}}{\partial t} = 0 = [\tilde{h} - \Omega \hat{J}_1, \tilde{\rho}]. \quad (8)$$

It seems thus that  $-(\Delta\kappa^* - \kappa\Delta^*)$  and  $-\left[\omega \hat{K}_1, \bar{\rho}\right]$  play a similar role provided that the value of the intrinsic angular velocity  $\omega$  is known for all  $\Omega$  (or  $I$ ). The main goal of the simple model described in this article is to find such a dependence without referring to cranking HFB calculations over the entire band. Now we could approach this aim by analyzing the results obtained in the previous article (I).

As shown there, the intensity of such counter-rotating currents (measured, e.g., by  $\langle \hat{K}_1 \rangle$ ) behaves as a function of the global rotation angular velocity  $\Omega$  in a very characteristic way. One may figure out that such a reactive mode of the fluid should be proportional to the excitation velocity field intensity (i.e.,  $\Omega$ ). Moreover it is also safe to assume that  $|\langle \hat{K}_1 \rangle|$  should be an increasing function of the pairing correlations measured by some power of  $-E_{\text{corr}}$  where  $E_{\text{corr}}$  is the (negative) pair correlation energy. Now, it is well known (see Ref. [7]) that pairing correlations tend to decrease upon increasing  $\Omega$ . When  $\Omega$  gets larger therefore, one should expect a balance between two competing phenomena resulting in a maximum of  $|\langle \hat{K}_1 \rangle|$  as a function of  $\Omega$  between two limiting cases. One is  $\Omega = 0$  and the other is obtained for a critical value  $\Omega_c$  corresponding to the alleged transition between a “superfluid” and a “normal” phase of nuclear matter.

The above described competition pattern has been illustrated in I by curves (see Figure 1 there) exhibiting  $\langle \hat{K}_1 \rangle$  as a function of  $\Omega$ . The main features of these results are sketched here in Figure 2 for the isoscalar values of  $\langle \hat{K}_1 \rangle$  in the three considered rotational bands (yrast superdeformed bands of  $^{150}\text{Gd}$  and  $^{192}\text{Hg}$ , and ground-state band of  $^{254}\text{No}$ ). As seen on this Figure, it is found only in the case of the  $^{192}\text{Hg}$  nucleus that the range of  $\Omega$  values spanned by our calculations (or more precisely by corresponding available experimental data)

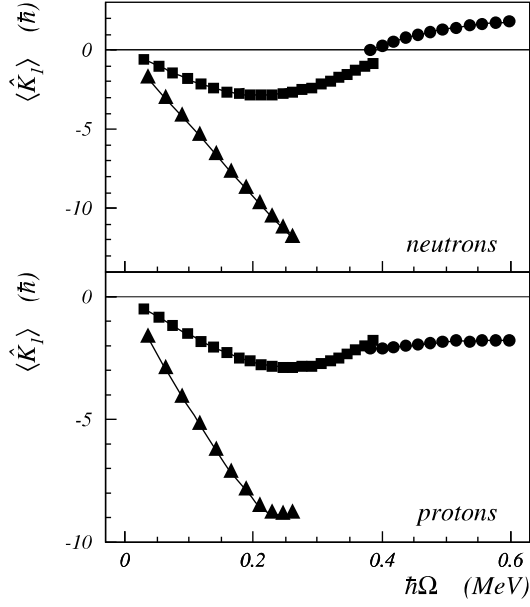


Figure 2. Kelvin circulation mean value in  $\hbar$  units for neutrons (upper panel) and protons (lower panel) in the three rotational bands studied in I. The convention in use is the following: circles for  $^{150}\text{Gd}$ , squares for  $^{192}\text{Hg}$  and triangles for  $^{254}\text{No}$ . Calculations are performed within the HFB formalism for  $^{254}\text{No}$  and within the HFB+LN formalism for  $^{150}\text{Gd}$  and  $^{192}\text{Hg}$ .

allows to exhibit a clean cut extremum in the corresponding curve. For the  $^{150}\text{Gd}$  nucleus one merely displays the up-going part of the curve (i.e., after the minimum of  $\langle \hat{K}_1 \rangle$  and before  $\Omega_c$ ) while, quite on the contrary, for the  $^{254}\text{No}$  nucleus, one only sees in Figure 2 the down-going part of the curve (i.e., just above  $\Omega = 0$ ) reaching its minimum, only for protons.

In addition, in the  $^{150}\text{Gd}$  case, a very interesting phenomenon is present and is worth discussing. As presented in I, one sees that substantial  $\langle \hat{K}_1 \rangle$  values are present for both neutrons and protons (namely about  $+1 \hbar$  and  $-2 \hbar$  respectively) even when pairing correlations have disappeared around  $\hbar\Omega = 0.6$  MeV. This phenomenon, also present for the proton Kelvin circulation in  $^{192}\text{Hg}$  (whose pairing correlations vanish around  $\hbar\Omega = 0.4$  MeV), is clearly a consequence of shell effects as it has been shown in I to be also present within purely rotating Routhian HF calculations.

Another way of representing the same trends is to plot, as done here in Figure 3 for the three considered nuclei, the values of the Lagrange multiplier  $\omega(\Omega)$  of the HF+V Routhian determined in I to obtain the relevant HFB  $\langle \hat{K}_1 \rangle$  values as a function of  $\Omega$ . As seen here they exhibit a parabolic-like behavior. Being

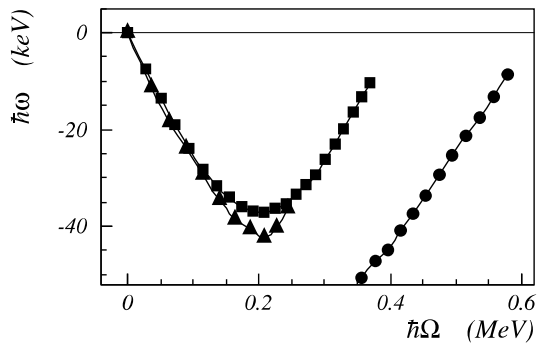


Figure 3. Kelvin circulation velocity  $\omega$  (in keV) as a function of the rotation angular velocity  $\Omega$  in MeV for the three nuclei considered in I and calculated within the constrained HF+V formalism. The symbol conventions are the same as those in Figure 2

related explicitly to the extra-contribution to  $\langle \hat{K}_1 \rangle$  due to pairing correlations, it is not surprising that such  $\omega(\Omega)$  curves are all located in our case in the  $\omega < 0$  part of the plane.

It is the aim of the present paper to understand quantitatively the pattern of these  $\omega(\Omega)$  curves. To put it in more operational terms we want to find whether we are able to deduce from the geometrical and pairing correlation properties of HFB solutions at zero-spin, the properties of rotational states. This of course would be only possible in cases where one deals with a “good” rotational band behavior, namely wherever the rotation does not couple significantly with other degrees of freedom like vibrations (e.g., no rotational stretching or anti-stretching) or single-particle excitations (e.g., no back-bending).

The paper will be organized as follows. In Section 2 we will briefly develop a simple magnetic-like model inspired from Ref. [7] using the well-known superconductor critical field concept (see, e.g., [8]) to describe the reduction of pairing correlations upon increasing  $\Omega$ . Section 3 will be devoted to the proposition and discussion of an ansatz for the relation between  $\omega$  and  $\Omega$ . We will present in Section 4, the prescriptions to determine the parameters of the above relation from the zero-spin HFB solution of a given nucleus. Finally, the validity of the model so established will be tested against actual HFB Routhian calculations for five nuclei (including the three already considered in I) and some conclusions will be drawn in Section 5.

## 2 A Simple Magnetic-Like Analog

In the simple model presented here (which is directly inspired from the rotational quenching mechanism of pairing correlations proposed by Mottelson and Valatin [7], the so-called Coriolis anti-pairing effect), we assume that the action of a global rotation on a pair of particles moving in opposite directions on a given

orbital may be described roughly in terms of two interacting magnetic dipoles ( $\vec{D}_1, \vec{D}_2$ ) plunged in an external magnetic field  $\vec{B}$ . The total energy of such a system is made of a term  $E_{\text{corr}}$  describing the dipole-dipole coupling and a term  $E_m$  taking into account the coupling with the external field. However, while the latter is understood as a magnetic field-dipole interaction term (see, e.g., Ref. [9], Chapter 5)

$$E_m = -\beta \vec{B} \cdot (\vec{D}_1 + \vec{D}_2); \quad \beta > 0, \quad (9)$$

the former does not originate, in our case, from a magnetic dipole-dipole interaction (which actually would tend to align  $\vec{D}_1$  and  $\vec{D}_2$ ), but rather from the strong interaction favoring quite on the contrary an anti-alignment of  $\vec{D}_1$  and  $\vec{D}_2$ . Therefore  $E_{\text{corr}}$  (which will be later called the correlation energy) is not given by the standard magnetic dipole-dipole expression (see, e.g., Ref. [9], Chapter 4) but rather, assuming the simplest possible form compatible with the physical requirements, as:

$$E_{\text{corr}} = \alpha (\vec{D}_1 \cdot \vec{D}_2 - |\vec{D}_1| |\vec{D}_2|); \quad \alpha > 0. \quad (10)$$

Assuming  $\vec{B}$  (whose norm will be denoted as  $B$ ) to lie on the 3-axis and  $\vec{D}_1$  to belong to the (1,3) plane, one gets for the total energy the following expression (where  $\theta_i, \phi_i$  are the usual spherical coordinates determining the  $\vec{D}_i$  direction):

$$E_{\text{tot}} = \alpha d^2 [\sin(\theta_1) \sin(\theta_2) \cos(\phi_2) + \cos(\theta_1) \cos(\theta_2) - 1] - \beta B d [\cos(\theta_1) + \cos(\theta_2)] \quad (11)$$

where  $d$  is the common norm of  $\vec{D}_1$  and  $\vec{D}_2$ .

The most stable equilibrium solution can be shown to corresponds to  $\theta_1 = \theta_2 = \theta$  and  $\phi_2 = \pi$  with

$$\cos \theta = \frac{\beta B}{2\alpha d}, \quad (12)$$

and the corresponding equilibrium energy

$$E_{\text{tot}} = -\alpha d^2 - \frac{\beta^2 B^2}{2\alpha}. \quad (13)$$

For the solution of Eq. (13), as expected, there is an upper limit for the norm  $B_c$  of  $\vec{B}$  given by

$$B_c = \frac{2\alpha d}{\beta} \quad (14)$$

corresponding to a full alignment ( $\theta = 0$ ). The corresponding correlation energy  $E_{\text{corr}}$  at equilibrium assumes the following form:

$$E_{\text{corr}} = 2\alpha d^2 \left[ \left( \frac{B}{B_c} \right)^2 - 1 \right]. \quad (15)$$

One may note, parenthetically, that the critical field value is obtained upon equating twice the correlation energy without field with the dipole magnetic interaction in the aligned case

$$-4\alpha d^2 = -\beta B d \quad (16)$$

which is very similar in spirit with the way in which one determines the critical magnetic field in the classical theory of superconductivity (see, e.g., Ref. [8]).

### 3 Model Assumptions in the Case of Nuclear Rotational States

As well known, the equations of motion of a particle coupled to a magnetic field by its charge, are similar to those of a massive particle moving in a rotating (non-inertial) frame upon identifying, with a proportionality constant, the magnetic field  $\vec{B}$  and the angular velocity  $\vec{\Omega}$ . It allows therefore to schematically model the coupling of a single-particle orbital motion in the rotating frame with the global rotation (in the laboratory frame) as the magnetic dipole interaction considered in the previous section [see Eq. (9)]. Similarly, the corresponding interaction energy between two particles moving in opposite directions on a same orbit could be approximated as:

$$E_{\text{corr}} = \lambda \left[ \left( \frac{\Omega}{\Omega_c} \right)^2 - 1 \right], \quad (17)$$

introducing thus a critical angular velocity  $\Omega_c$  which will be defined below.

The preceding could pertain, a priori, to the description of the internal and external energies of a single pair. It is our contention, however, that such a quantity behaves, up to a multiplicative constant, as the energies of all the pairs to be considered in the nucleus. Therefore, after suitably redefining the phenomenological parameter  $\lambda$ , one may consider the expression above given in Eq. (17) as the total nuclear pairing correlation energy.

Now, we are proceeding with the major assumption behind our model. Namely, we assume that the vector  $\vec{\omega}$  associated with the intrinsic vortical motion is proportional to the global rotation angular velocity  $\vec{\Omega}$ . The corresponding proportionality factor is negative and we assume that its absolute value is an increasing function of the total correlation energy of Eq. (17). Specifically, we propose that the projection  $\omega$  of the vector  $\vec{\omega}$  on the vector  $\vec{\Omega}$  is given by:

$$\omega = -\alpha(E_{\text{corr}})\Omega; \quad \alpha > 0. \quad (18)$$

Upon inserting in such an ansatz, the correlation energy expression of Eq. (17), one gets for  $\omega$

$$\omega = -k\Omega \left[ 1 - \left( \frac{\Omega}{\Omega_c} \right)^2 \right]; \quad k > 0 \text{ and } \Omega \in [0, \Omega_c]. \quad (19)$$

One gets two extrema for  $\omega$  corresponding to:

$$\Omega = \frac{\Omega_c}{\sqrt{3}} \quad (20)$$

The correlation energy associated with this solution, expressed in units of its value at zero angular momentum ( $\Omega = 0$ ) is:

$$\frac{E_{\text{corr}}(\Omega)}{E_{\text{corr}}(0)} = \frac{2}{3}. \quad (21)$$

#### 4 Determination of the Model Parameters

Let us summarize the modeling which has been performed so far. With Eq. (19), we have a three-parameter expression for the intrinsic vorticity parameter  $\omega$  in terms of the global rotation angular velocity  $\Omega$ , namely:

- i) a scale parameter ( $\Omega_c$ ) for the abscissa variable  $\Omega$ ,
- ii) a scale parameter ( $k$ ) for the studied quantity  $\omega$ .

The former parameter  $\Omega_c$  may be fixed a priori for each considered nucleus as sketched before. In Eq. (16), it is given upon equating twice the correlation energy without field (thus, here, without rotation), with the equivalent of the dipole-magnetic coupling energy in the aligned case, namely the rotational energy without pairing. We therefore get

$$\Omega_c = \sqrt{\frac{4E_{\text{corr}}(\Omega = 0)}{\mathfrak{S}_{\text{ETF}}}}, \quad (22)$$

where  $\mathfrak{S}_{\text{ETF}}$  is the semiclassical (Extended Thomas-Fermi) moment of inertia of an unpaired nucleus using the same effective interaction at the relevant deformation.

In most current Routhian HFB calculations (including ours [10]) using the Skyrme interaction for the “normal” mean field, there is an inconsistency in the interaction used in the Hartree-Fock (“normal”) part and in the part dealing with pairing correlations. As a result, the naturally defined correlation energy, namely the energy difference between the correlated and the non-correlated solutions, is not relevant. Thus we must replace in Eq. (22), the correlation energy  $E_{\text{corr}}(\Omega = 0)$  by an unequivocal quantity. The “abnormal” part of the total HFB energy – sometimes called (see, e.g., Ref. [11]) the “pair condensation energy”,  $E_{\text{cond}}$  – could be considered in practice in this case, as a more reliable index of the amount of pairing correlations. As demonstrated in model calculations performed in the three cases considered in I according to the approach of Ref. [12] which is free from the usual HFB breaking of the particle number symmetry, the

pair condensation energy is found to be roughly equal to twice the pair correlation energy. The Eq. (22) yielding the critical value  $\Omega_c$  becomes thus

$$\Omega_c = \sqrt{\frac{2E_{\text{cond}}(\Omega = 0)}{\mathfrak{S}_{\text{ETF}}}}. \quad (23)$$

The scale parameter  $k$  can be determined in the following way. If we assume that our relation  $\omega(\Omega)$  is of any global relevance, it should also be valid in the low angular velocity regime. Namely, one should have for  $\Omega \ll \Omega_c$ :

$$k = -\frac{\omega}{\Omega}. \quad (24)$$

In this adiabatic regime, one obtains an expression for the total collective kinetic energy in a HF+V approach which is quadratic in  $\Omega$  and  $\omega$ , as with the notation of Ref. [13]

$$E(\Omega, \omega) = \frac{1}{2} (A\omega^2 + 2B\omega\Omega + C\Omega^2). \quad (25)$$

Upon including the above limiting expression for the ratio of  $\omega$  and  $\Omega$  one gets the expectation value of the total angular momentum as

$$\langle \hat{J}_1 \rangle = \left. \frac{\partial E(\Omega, \omega)}{\partial \Omega} \right|_{\omega = -k\Omega} = (C - kB) \Omega, \quad (26)$$

which in turn yields the value of the dynamical moment of inertia within our model:

$$\mathfrak{S}_{\text{mod}}^{(2)} = \frac{d \langle \hat{J}_1 \rangle}{d\Omega} = C - kB. \quad (27)$$

Now, we define the HFB Routhian dynamical moment of inertia  $\mathfrak{S}_{\text{HFB}}$  (in the low angular velocity regime) and require it has the same value as  $\mathfrak{S}_{\text{mod}}^{(2)}$ :

$$\mathfrak{S}_{\text{HFB}} = \frac{\langle \hat{J}_1 \rangle}{\Omega} = \mathfrak{S}_{\text{mod}}^{(2)}. \quad (28)$$

One is left therefore, now, with the problem of determining the moments  $A$ ,  $B$  and  $C$ . A natural way to do so would be to calculate the total energy surface as a function of  $\Omega$  and  $\omega$  in the vicinity of zero for both parameters through doubly constrained HF calculations (called in I Routhian HF + V calculations) and then perform a quadratic fit.

Instead, we have evaluated them from the single-particle eigenstates of the corresponding static Hartree-Fock solution through the Inglis cranking formula [14, 15] where the cranking operators are (see Ref. [13]) the first components of the total angular momentum  $\hat{J}_1$  and of the Kelvin circulation operator  $\hat{K}_1$ . With

usual notation one has thus

$$C = 2 \sum_{p,h} \frac{|\langle p|\hat{J}_1|h\rangle|^2}{\epsilon_p - \epsilon_h}, \quad B = 2 \sum_{p,h} \frac{\langle p|\hat{J}_1|h\rangle \langle h|\hat{K}_1|p\rangle}{\epsilon_p - \epsilon_h},$$

$$A = 2 \sum_{p,h} \frac{|\langle p|\hat{K}_1|h\rangle|^2}{\epsilon_p - \epsilon_h}. \quad (29)$$

However it is well known (see e.g. Ref. [16]) that these mass parameters lack the so-called Thouless-Valatin [17] terms which are merely coming from the time-odd density response to the self-consistent time-odd Hartree-Fock mean field. They have been therefore multiplied by a  $(1 + \eta)$  corrective term as it has been proposed in Ref. [18] for the usual cranking moment  $C$ . As we will see in the next section, two different Skyrme effective interactions have been used in our calculations (SIII [19] and SkM\* [20]). The corresponding values for  $\eta$  are 0.2 and 0.1 respectively.

As a result one gets the following value for  $k$ :

$$k = \frac{C - (1 - \eta)\mathfrak{S}_{\text{HFB}}}{B}. \quad (30)$$

## 5 Results and Conclusions

We have applied the previously described protocol to define the model parameters  $\Omega_c$  and  $k$  [see Eq. (19)] for rotational bands in five nuclei, including the three cases studied in I and adding the ground-state bands of  $^{154}\text{Sm}$  and  $^{178}\text{Hf}$ . The Kelvin circulation mean values for protons and neutrons calculated in the Routhian HFB approach are plotted on Figure 4 as a function of  $\Omega$  for these two nuclei. The different trends of these curves for  $^{154}\text{Sm}$  as opposed to  $^{178}\text{Hf}$  do not reflect the behavior (illustrated on Figure 5) of the condensation energies, but some specific dynamical properties which will be discussed below.

It is generally considered (see, e.g., [12]) that the SIII [19] interaction provides extremely good spectroscopic properties for normally deformed nuclei, while the SkM\* [20] interaction, due to its better surface tension, is well suited to the description of superdeformed or heavy (i.e., with a fissility close to 1) nuclei. Therefore we have used the former for the calculations of the ground-state bands of  $^{154}\text{Sm}$  and  $^{178}\text{Hf}$ , and the latter for the three others nuclei already considered in I.

First, we have obtained values of the critical angular velocities  $\Omega_c$  according to Eq. (23).

For the five nuclei, HFB calculations at zero-spin have been performed to yield the corresponding pair condensation energies  $E_{\text{cond}}(\Omega = 0)$ . They have already been shown on Figure 2 in I for  $^{192}\text{Hg}$  and  $^{254}\text{No}$ . In the  $^{150}\text{Gd}$  case,

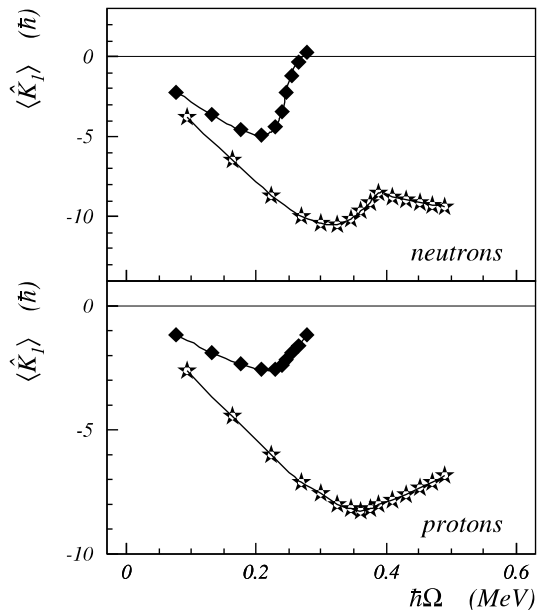


Figure 4. Same as Figure 2 for  $^{154}\text{Sm}$  (diamonds) and  $^{178}\text{Hf}$  (stars).

we have “artificially” constructed a zero-spin solution consistent with the deformation of the superdeformed band under consideration by constraining the HFB solution to have the value of the axial mass quadrupole moment of the SD rotational band states (of course, without constraint one would have obtained the normally deformed  $^{150}\text{Gd}$  equilibrium solution).

The values of  $\mathfrak{S}_{HFB}$  have been calculated in the close vicinity of  $\Omega = 0$  and may be deduced from the plots of  $\mathfrak{S}^{(2)}$  of Figure 1 in I for  $^{192}\text{Hg}$  and  $^{254}\text{No}$ . Again in the case of  $^{150}\text{Gd}$  this value is yielded by a Routhian HFB calculation with an appropriate constraint on the axial mass quadrupole moment (as above discussed). Finally the  $k$  parameter is determined using Eq. (30).

As a result, the curves  $\omega(\Omega)$  yielded by the above defined parameters are plotted on Figures 6–8 in comparison with the self-consistently calculated ones (HF+V). The global agreement is rather satisfactory in a qualitative fashion for  $^{150}\text{Gd}$ ,  $^{192}\text{Hg}$  and  $^{254}\text{No}$ . This is not so for  $^{154}\text{Sm}$  and  $^{178}\text{Hf}$  where a sudden raise of  $\omega$  occurs. In these three figures, experimental data are taken from Refs. [21] for  $^{154}\text{Sm}$  and  $^{178}\text{Hf}$ , [22] for  $^{150}\text{Gd}$ , [23] for  $^{192}\text{Hg}$  and [24–26] for  $^{254}\text{No}$ .

The final step of the assessment of our model consists of course in performing Routhian HF+V calculations with the model values of  $\omega(\Omega)$  and compare their results with those of corresponding Routhian HFB calculations. They

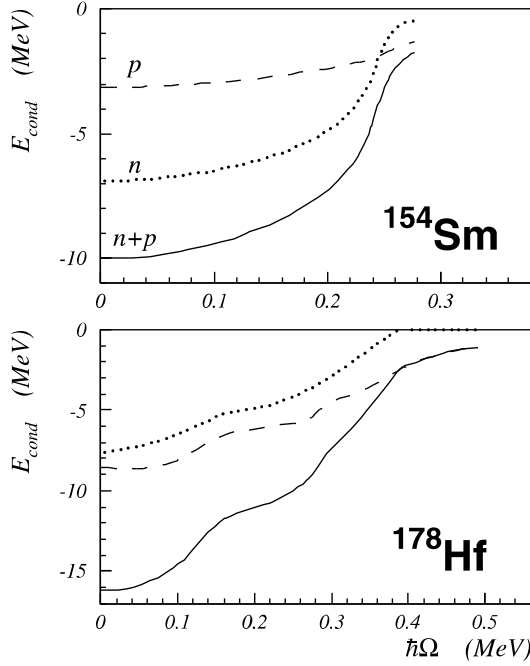


Figure 5. Condensation energies (in MeV) as functions of the angular velocity  $\Omega$  (in MeV) for  $^{154}\text{Sm}$  (upper panel) and  $^{178}\text{Hf}$  (lower panel). Proton (neutron resp.) condensation energies are represented as a dashed line (dotted line resp.) and the total condensation energy is represented as a full line. Calculations are performed within the HFB formalism.

should also be compared with the results of Routhian HF+V calculations where the constrained  $\langle \hat{K}_1 \rangle$  expectation values are those obtained in Routhian HFB calculations. However we knew already from I (see Figure 1 therein) that both are very close indeed.

The results of the comparison fall into three categories. For the  $^{192}\text{Hg}$  and  $^{254}\text{No}$  nuclei (Figure 6), the agreement between the HFB (and thus HF+V) and the model results are very good indeed. One exception however should be noted, it concerns the high spin part of the superdeformed band of  $^{192}\text{Hg}$  where pairing correlations are strongly damped or disappearing in the HFB approach and therefore the simple ansatz here is obviously lacking any sound basis.

The  $^{154}\text{Sm}$  and  $^{178}\text{Hf}$  cases (Figure 7) are interesting in that HFB calculations exhibit a up-bending pattern for both  $\mathfrak{S}^{(1)}$  and  $\mathfrak{S}^{(2)}$ . The fact that it corresponds very well to the experimental situation in the latter and is completely absent in the data for the former is irrelevant for our discussion here. It is remarkable that our model just ignores these bendings. Therefore we must con-

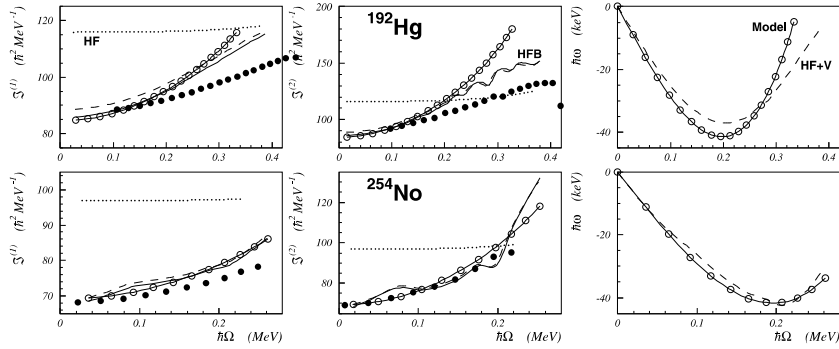


Figure 6. Results of our calculations for  $^{192}\text{Hg}$  (upper panels) and  $^{254}\text{No}$  (lower panels). From left to right we show (as functions of the rotation angular velocity  $\Omega$  in MeV) for each nuclei the kinetic moment of inertia and the dynamical moment of inertia (in  $\hbar^2 \text{MeV}^{-1}$  units) as well as the Kelvin circulation velocity  $\omega$  (in keV). The results obtained within various formalisms are represented as follows: dotted line for the (pure) HF formalism, full line (dashed line resp.) for the HFB (HF+V resp.) formalisms and full line with opened circles for our model. Experimental data for the moments of inertia are represented as filled circles. The Lipkin-Nogami correction has been applied for the Hg isotope.

clude that these patterns are not to be attributed to a pairing-rotation coupling but to something else which is (as well known) the intrusion of quasiparticle degree of freedom in the rotational dynamics.

As for the last nucleus of our study ( $^{150}\text{Gd}$ ), Figure 8 displays clearly in its  $\mathfrak{S}^{(1)}$  and  $\mathfrak{S}^{(2)}$  parts that obviously the quasiparticle degrees of freedom are dominating there in explaining the rotational behavior within this superdeformed band. Nevertheless, it is to be noted that our model works fairly well in the low

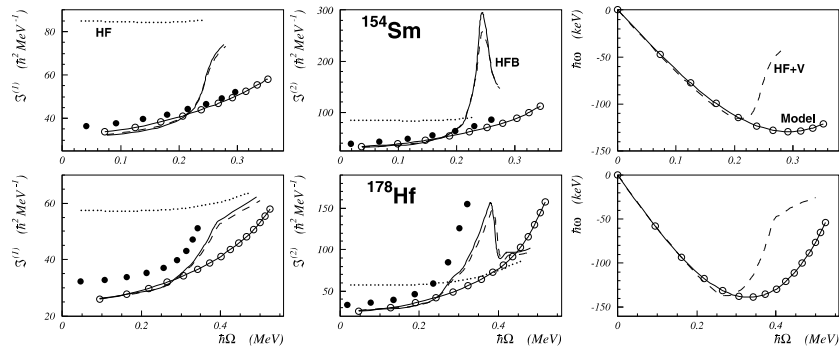


Figure 7. Same as Figure 6 for  $^{154}\text{Sm}$  (upper panels) and  $^{178}\text{Hf}$  (lower panels).

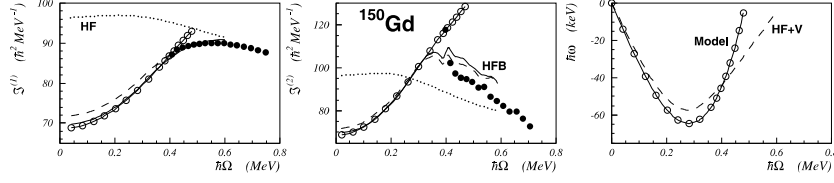


Figure 8. Same as Figure 6 for  $^{150}\text{Gd}$ . The Lipkin-Nogami correction has been applied.

angular velocity regime and only fails above  $\hbar\Omega \simeq 0.4$  MeV after the occurrence of a change in the ordering of quasiparticle states.

Let us summarize what has been learned from such a comparison. Actually, one should conclude at two different levels.

First of all, it appears in some of the studied cases that one could skip Routhian HFB calculations at finite values of the angular momentum and replace them by more handy constrained Routhian HF calculations. For that one needs only to perform a HFB calculation in the close vicinity of  $\Omega = 0$ . This result is of some practical value in that it allows to predict quickly what could be the trend of the moments of inertia with respect to the angular velocity.

However, the limitation of such an approach is clear. It is only valid in cases where the rotational (global) collective mode does not couple either with deformation modes (no rotational stretching, anti-stretching or triaxial modes, etc.) nor with single-particle degrees of freedom (no back-bending for instance). It is only able to give an account which turns out to be rather good quantitatively of the coupling of the pairing degrees of freedom with the rotational mode.

Taking at face value the rough assumption made in previous papers [1, 4] that the collective effects of these correlations could be mocked up by Chandrasekhar  $S$ -type ellipsoid velocity fields together with the Mottelson-Valatin picture [7] for the rotational quenching of pairing correlations, our model provides a good reproduction of fully self-consistent HFB results. It offers thus reasonable grounds to assume that both conjectures rather accurately describe the microscopic coupling at work in rigidly deformed purely collective rotational bands.

A short summary of this work may be formulated into the following way:

1. The pairing part  $-(\Delta\kappa^* - \kappa\Delta^*)$  in the relevant HFB equations shown in Eq. (6) describes very well the behavior of the rotating paired systems except in the low pairing regions. This term introduces intrinsic vortical currents in the plane perpendicular to the rotational axis and therefore is changing the moments of inertia of the system. The problem in the low pairing regions consist in the right determination of the pairing matrix  $\kappa$  and the gap potential  $\Delta$  at higher angular momenta. This must be done in a selfconsistent way by the full system of HFB equations. Due to the

deficiencies from its quasiparticle nature, the HFB approach is not able to reproduce in a correct way the number of particles and thus the right gap potential for weakly coupled Cooper pairs.

2. When one replaces the term  $-(\Delta\kappa^* - \kappa\Delta^*)$  in the relevant HFB equations (Eq. (6)) by the term  $-\left[\omega\widehat{K}_1, \bar{\rho}\right]$  one obtains the equations of motion of the HF+V approach (Eq. (7)). It generates intrinsic vortical currents in the cranked HF solutions, which have the same effects on the moment of inertia as the  $-(\Delta\kappa^* - \kappa\Delta^*)$  term (in condition that the HF+V solution is sharing the same  $\widehat{K}_1$  as the HFB one). The equivalence of the so-obtained moments of inertia does not lead to equivalent single-particle states. Whether the HF+V single particle-states are better or worse the HFB ones, this could be explored in an additional study, by comparing the transition probabilities of the HFB and HF+V approaches with the experiment. The question of the determination of the right values of  $\omega$  in the additional term-constraint  $-\left[\omega\widehat{K}_1, \bar{\rho}\right]$  remains, and it is solved through the simple model introduced here.
3. The simple model proposed in this paper helps to determine the right amount of counterrotating S-ellipsoidal currents in rotating nuclei. We have found a relation between the angular velocity  $\Omega$  and the intrinsic angular velocity  $\omega$ , which seems to be universal for the cases where the dynamics is restricted to the coupling between the global rotation and the intrinsic vortical modes. This is a very simple and phenomenological approach. It is relying on the known theoretical information for a given rotational band at  $\Omega = 0$ . In this way it provides the moments of inertia of the band due to the increase of the velocity of the rotation. In the studied cases this provides the right moments of inertia, whenever a band crossing is nonexistent. At higher angular momenta, when there is a band crossing, this approach is not able to “switch” to the new (now Yrast) band because the initial information which gave the parameters of the model are now valid for the excited band.

This model is giving us a further insight and understanding in the current dynamics and the nature of the pairing correlations. Further, this model yields a sound ground base for evaluation of the coupling of rotation with other modes (shape distortions, quasiparticle degrees of freedom).

### **Acknowledgments**

One of the authors (Philippe Quentin) would like to thank the Theoretical Division of the LANL for the hospitality extended to him during his stay at Los Alamos. Part of this work has been funded through an agreement (# 12533)

between the BAS (Bulgaria) and the CNRS (France) and another through an agreement between the JINR (Russia) and the IN2P3/CNRS (France) which are gratefully acknowledged.

## References

- [1] H. Lafchiev, D. Samsøen, P. Quentin and I. N. Mikhailov (2003) *Phys. Rev. C* **67** 014307.
- [2] I. N. Mikhailov, P. Quentin and D. Samsøen (1997) *Nucl. Phys. A* **627** 259.
- [3] D. Samsøen, P. Quentin and J. Bartel (1999) *Nucl. Phys. A* **652** 34.
- [4] D. Samsøen, P. Quentin and I. N. Mikhailov (1999) *Phys. Rev. C* **60** 014301.
- [5] G. Rosensteel (1992) *Phys. Rev. C* **46** 1818.
- [6] S. Chandrasekhar (1987) *Ellipsoidal Figures of Equilibrium* (Dover, New York).
- [7] B. R. Mottelson and J. G. Valatin (1960) *Phys. Rev. Lett.* **5** 511.
- [8] C. Kittel (1963) *Quantum Theory of Solids* (Wiley, New York).
- [9] J. D. Jackson (1962) *Classical Electrodynamics* (Wiley, New York).
- [10] H. Lafchiev, D. Samsøen, P. Quentin and J. Piperova (2001) *Eur. Phys. J A* **12** 155.
- [11] H. Flocard, P. Quentin, A. K. Kerman and D. Vautherin (1973) *Nucl. Phys. A* **203** 433.
- [12] N. Pillet, P. Quentin and J. Libert (2002) *Nucl. Phys. A* **697** 141.
- [13] I. N. Mikhailov and P. Quentin (1995) *Phys. Rev. Lett.* **74** 3336.
- [14] D. R. Inglis (1954) *Phys. Rev.* **96** 1059.
- [15] D. R. Inglis (1956) *Phys. Rev.* **103** 1786.
- [16] M. J. Giannoni and P. Quentin (1980) *Phys. Rev. C* **21** 2060.
- [17] D. J. Thouless and J. G. Valatin (1962) *Nucl. Phys.* **31** 211.
- [18] J. Libert, M. Girod and J.-P. Delaroche (1999) *Phys. Rev. C* **60** 054301.
- [19] M. Beiner, H. Flocard, N. Van Giai and P. Quentin (1975) *Nucl. Phys. A* **238** 29.
- [20] J. Bartel, P. Quentin, M. Brack, C. Guet and H.-B. Håkansson (1982) *Nucl. Phys. A* **386** 79.
- [21] R. B. Firestone *et al.* (1996) *Table of isotopes, eighth edition* (J. Wiley and sons, New York) and Refs. quoted therein.
- [22] P. Fallon *et al.* (1991) *Phys. Lett. B* **257** 269.
- [23] B. Gall *et al.* (1994) *Z. Phys. A* **347** 223.
- [24] P. Reiter *et al.* (1999) *Phys. Rev. Lett.* **82** 509.
- [25] M. Leino *et al.* (1999) *Eur. Phys. J. A* **6** 63.
- [26] P. Reiter *et al.* (2000) *Phys. Rev. Lett.* **84** 3542.